

## Analysis and Implementation of a High Boost Ratio DC-DC Converter for Minimizing Commutation Torque Ripple in Brushless DC Motor

M. Senthil Raja, B. Geethalakshmi

Departement of Electrical and Electronics Engineering, Pondicherry Engineering College, India

---

### Article Info

#### Article history:

Received Nov 21, 2015  
Revised May 13, 2016  
Accepted May 31, 2016

#### Keyword:

Brushless dc motor (BLDC)  
Commutation  
DC-link voltage strategy  
High boost ratio converter  
Torque ripple

---

### ABSTRACT

Brushless dc motor still suffers from commutation torque ripple, which primarily depends on transient line current in the commutation interval. In order to control the incoming and outgoing phase currents to change at the same rate during commutation, this paper presents a novel high boost ratio DC-DC circuit topology in the front end of the inverter. With a suitable closed loop control scheme, the proposed high boost ratio DC-DC converter is operated with two different duty ratios one during commutation period and the other during non commutation period. The cause of commutation ripple is analyzed, and the way to adjust the duty ratio for obtaining the desired dc link voltage is introduced in detail. Finally, simulation and experimental results show that, compared with the existing dc-dc converter topologies, the proposed method can obtain the desired voltage much faster and minimize commutation torque ripple more efficiently.

Copyright © 2016 Institute of Advanced Engineering and Science.  
All rights reserved.

---

### Corresponding Author:

M. Senthil Raja  
Departement of Electrical and Electronics Engineering,  
Pondicherry Engineering College,  
Pondicherry14, India.  
Email: muthappa.senthil@yahoo.com

---

## 1. INTRODUCTION

Brushless dc motors (BLDCM) possessing simple structure, high power density, high torque/current ratio, robustness, and better dynamics have been widely used in all kinds of areas, such as electric vehicles, robotics, small actuators, industry and automotive electronics [1]–[3]. The performance of such motors has been significantly improved due to the great development of power converters, magnetic performance of magnets, and motion control technology in recent years [4]–[6]. However, commutation torque ripple has always been one major factor in preventing BLDCM from achieving high performance. The causes for torque ripple in BLDCM are the imperfection of motor design and manufacture, non-ideal EMF and unequal current sharing between the phases during commutation [7] and [8]. Since torque smoothness is an essential requirement for such high-performance applications, a wide variety of techniques have been proposed by many researchers during the past two decades to minimise the torque ripple [9]–[14].

In recent years, multilevel inverters have gained much attention in the application areas of BLDC motor drives [21]. The problem of imperfection in the motor design is overcome in [13] and [14], wherein [13] suggests application of Taguchi method in designing the shape of permanent magnets and in [14] a segmented permanent magnet structure is proposed which significantly reduced the commutation torque ripple. Some researches [3], [15] – [17] introduced novel power converter topologies and PWM techniques for controlling the input voltage of the BLDCM drive. In [3], the inverter is operated in 120° mode for lower speed range of the machine and in 180° mode for higher speed range thereby optimizing the commutation

torque ripple. In [15], a buck converter is used for reducing the commutation torque ripple at low speed. In [16], a superlift Luo converter is placed at the input stage of the inverter to produce desired dc link voltage, and the structure works more effectively under high-speed operating condition, compared with the method proposed in [15]. However the methods proposed in [15] and [16] suffer from slow voltage adjustment, and therefore, they can only achieve satisfactory torque pulsation suppression in low- or high-speed regions. This problem is alleviated in [17], [20] whereby a SEPIC converter with a switch over MOSFET is used to implement the dc link voltage adjustment. However, the power converter requires a very high direct dc voltage as input during non-commutation period and another boosted voltage boosted through SEPIC converter during the commutation period. For such dc voltage adjustment, this circuit requires an additional switch selection circuit for switching from non commutation period to commutation period.

Use of low voltage input source is preferred over a high voltage source, and hence in the present paper a high boost ratio dc – dc converter (HBDC) [18] that requires very low dc voltage at the input side is used. Of the entire high-boost ratio non-isolated DC–DC converter topologies published [19], a combination of fly-back and boost converter is highly efficient as it increases the boost ratio with lower cost and greater efficiency [18]. Besides, in the proposed topology, the need of an additional switch selection circuit as used in [17] is overcome by operating the converter with two different duty ratios one during non-commutation period, and the other during commutation period. Simulation and experimental results show that compared with common the dc–dc converter topologies, the proposed converter operated with suitable duty ratio control can reduce commutation torque ripple significantly.

## 2. PROPOSED HIGH BOOST RATIO DC-DC CONVERTER AND ITS OPERATION

In the proposed high-boost ratio DC-DC converter [18] shown in Figure.1, HT is a hybrid transformer with turns ratio 1: n,  $M_1$  is the MOSFET switch carrying current  $I_{s1}$  and  $C_{in}$  is the input capacitor. A coupled inductor has been employed in the primary side of the transformer to provide a high step-up ratio and to reduce the switch voltage stress substantially.  $D_1$  is the clamping diode, which provides current path for the leakage inductance of the hybrid transformer when  $M_1$  is OFF.  $C_c$  is the clamping capacitor which captures the leakage energy from the hybrid transformer and transfers it to the resonant capacitor  $C_r$ , which is connected in series with the hybrid transformer.

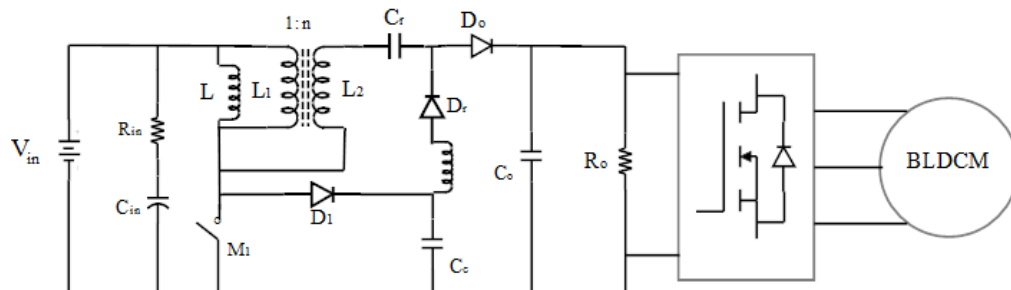


Figure 1. Configuration of BLDCM driving system with a high boost ratio dc-dc converter

The resonant circuit comprises of  $C_c$ ,  $C_r$ ,  $L_r$  and  $D_r$ , where  $L_r$  is the resonant inductor which operates in the resonant mode and  $D_r$  is the resonant diode which is used to provide a uni-directional current flow path for the operation of the resonant circuit. The conduction of  $D_r$  is determined by the state of the active switch  $M_1$ ,  $D_o$  is the output diode similar to the coupled-inductor boost converter,  $C_o$  is the output capacitor and  $R_L$  is the resistive load.  $I_{cr}$  is the current of the resonant capacitor  $C_r$ ,  $I_{in}$  is the primary side current of hybrid transformer and  $I_o$  is the output diode current.

The steady state topology stages of the proposed DC-DC converter for one switching cycle can be given in five stages. The explanation of each mode is as follows:

### Mode 1: ( $t_0 < t < t_1$ )

The equivalent circuit corresponding to this mode is shown in Figure. 2 in which the MOSFET  $M_1$  is switched ON, the primary side voltage of hybrid transformer is charged to input voltage  $V_{in}$ .  $C_r$  is charged by  $C_c$ , which was charged in a previous cycle. The input voltage is reflected on the secondary side of the hybrid transformer by n-times ( $nV_{in}$ ), due to the magnetic coupling between the primary and secondary windings. The energy stored in the capacitor  $C_c$  is transferred to  $C_r$ , which in-turn is transferred to the load

when MOSFET is turned OFF. The current in MOSFET  $M_1$  is the sum of the resonant current  $I_r$  and linear magnetising inductor current.

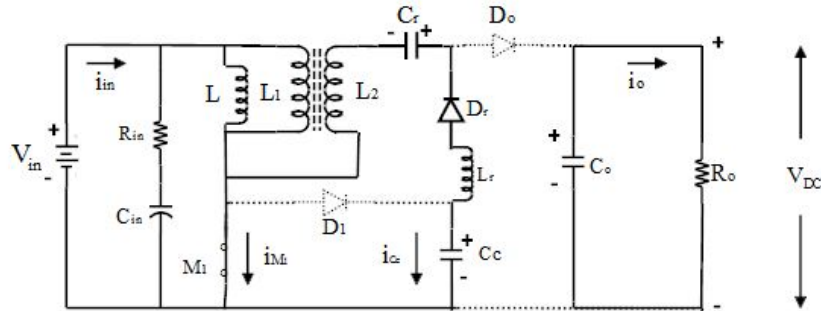


Figure 2. Mode 1 Equivalent circuit

**Mode 2: ( $t_1 < t < t_2$ )**

In this mode, the MOSFET  $M_1$  is turned OFF as depicted in Figure 3(a) and therefore the clamping diode  $D_1$  is turned ON by the leakage energy stored in the hybrid transformer during mode 1. Clamping capacitor  $C_c$  is charged during this period. This causes the voltage to be clamped

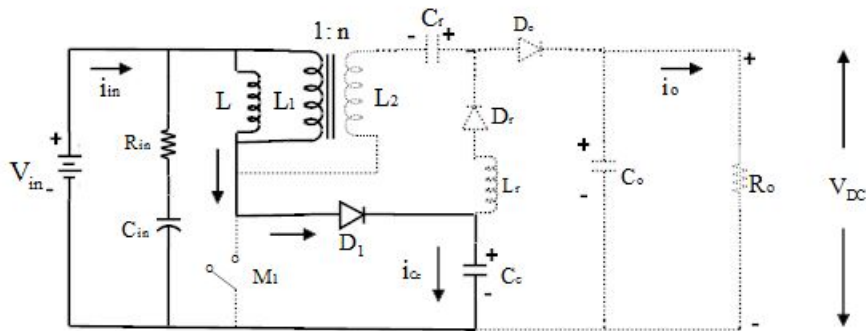


Figure 3(a). Equivalent circuit Mode 2

**Mode 3: ( $t_2 < t < t_3$ )**

The clamping capacitor  $C_c$  is charged to voltage that can forward bias the output diode  $D_o$ . So the energy stored in the magnetising inductor and capacitor ( $C_r$ ) is being transferred to the load. The clamp diode  $D_1$  continues to conduct while  $C_c$  remains charged. This process continues until  $C_c$  gets discharged and the corresponding equivalent circuit is shown in Figure 3(b).

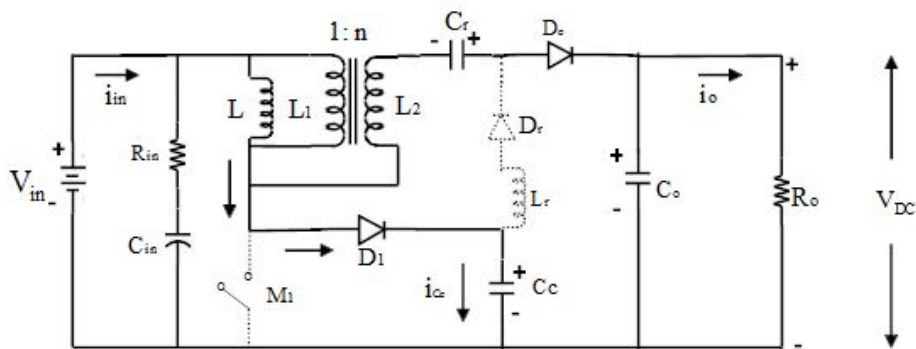


Figure 3(b). Equivalent circuit Mode 3

**Mode 4: ( $t_3 < t < t_4$ )**

When  $C_c$  gets discharged, the diode  $D_1$  is reverse biased and as a result the energy stored in the magnetising inductor of the hybrid transformer and the capacitor  $C_r$  is simultaneously transferred to the load. During the steady state operation, the charge through  $C_r$  must satisfy the charge balance. It is observed that the capacitor operates in hybrid-switching mode (i.e.) by having charged in resonant mode and discharged linearly and is clear from the equivalent circuit is shown in Figure 3(c).

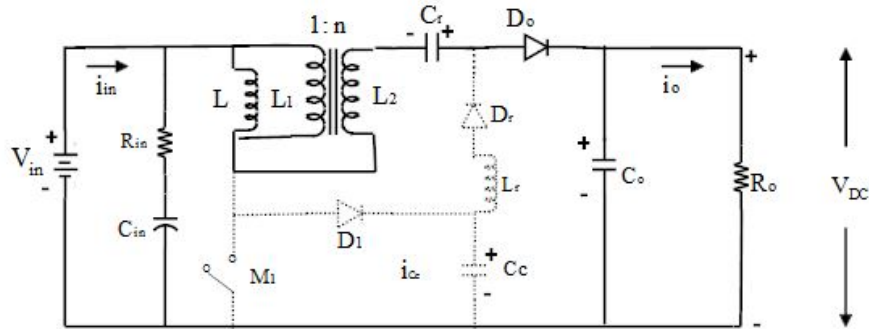


Figure 3(c). Equivalent circuit Mode 4

**Mode 5: ( $t_4 < t < t_0$ )**

The MOSFET  $M_1$  is turned ON at time  $t_4$  and the corresponding equivalent circuit is given in Figure 4. The output diode current  $I_0$  continues to flow for a short time due to the leakage effect of the hybrid transformer. The diode  $D_0$  will be reverse biased at time  $t_0$ ; the next cycle starts.

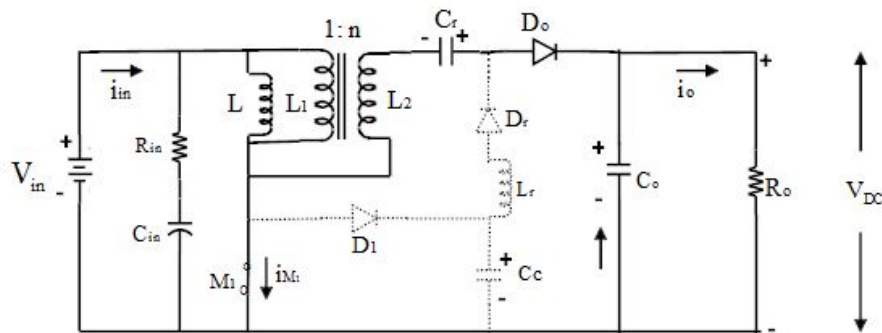


Figure 4. Equivalent circuit Mode 5

**3. ANALYSIS OF COMMUTATION TORQUE RIPPLE IN BLDCM**

BLDCM conventionally operates in two phase  $120^\circ$  (electrical) conducting mode, and this conducting mode includes a commutation region and a non commutation region. This paper focuses on the commutation region, aiming at reducing commutation torque ripple. For the current analysis, it is assumed that the motor is unsaturated, armature reaction is negligible, stator winding is symmetrical, the resistances and inductances of the motor windings are constant and the motor exhibits no cogging torque. The voltage equation for the BLDC motor can be represented by (1) [8] and [17]

$$\begin{aligned}
 v_a &= i_a R + L \frac{di_a}{dt} + e_a + v_{no} \\
 v_b &= i_b R + L \frac{di_b}{dt} + e_b + v_{no} \\
 v_c &= i_c R + L \frac{di_c}{dt} + e_c + v_{no}
 \end{aligned}
 \tag{1}$$

Where  $v_a, v_b$  and  $v_c$  are the phase voltages of the three windings of BLDC motor,  $i_a, i_b$  and  $i_c$  are the phase currents,  $e_a, e_b$  and  $e_c$  are the trapezoidal back emf,  $L=L_s - M$  is the equivalent inductance of the phase windings and R is the resistance of the phase windings. The torque equation of the BLDCM [17] is

$$T_e = \frac{(e_a i_a + e_b i_b + e_c i_c)}{\omega_r} \quad (2)$$

Where  $\omega_r$  is the speed of the motor.

The presence of inductance elements in the phase windings results in a trapezoidal current waveform instead of rectangular one. This leads to torque ripple during commutation periods. Before the commutation interval, the current flows through phase-A to phase-C as shown in Figure 5.(a). After the commutation interval, the current flows through phase-B to phase C which is shown in Figure 5(b).

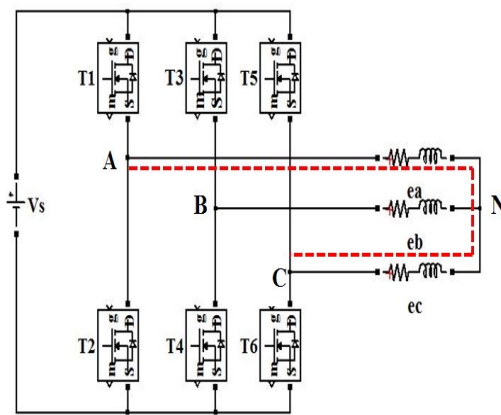


Figure 5(a) Conducting stage of phase-A and phase-C

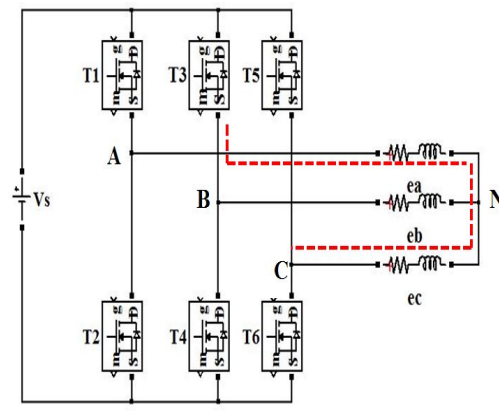


Figure 5(b) Conducting stage of phase-B and phase-C

For this analysis, the commutation of the current from phase A to phase B is considered. Then the initial voltage values at the beginning of commutation can be drawn as follows:

At the instant of commutation,

$$V_a = 0; V_b = V_{dc}; V_c = 0$$

$$e_a = 0; e_b = E_m; e_c = -E_m$$

(3)

Applying the initial conditions given in (3) to (1) and (2),

$$0 = i_a R + L \frac{di_a}{dt} + E_m + v_{no}$$

$$V_{dc} = i_b R + L \frac{di_b}{dt} + E_m + v_{no}$$

$$0 = i_c R + L \frac{di_c}{dt} - E_m + v_{no}$$

(4)

$$T_{e0} = 2 \frac{E_m I_m}{\omega_r}$$

(5)

With the phase resistance neglected in (4), then the rate of change of phase currents can be expressed as

$$\begin{aligned}\frac{di_a}{dt} &= \frac{-(V_{dc} + 2E_m)}{3L} \\ \frac{di_b}{dt} &= \frac{2(V_{dc} - E_m)}{3L} \\ \frac{di_c}{dt} &= \frac{-(V_{dc} - 4E_m)}{3L}\end{aligned}\quad (6)$$

During commutation the torque is obtained as

$$T_e = \frac{2E_m}{\omega_r} \left( I_m + \frac{V_{dc} - 4E_m}{3L} t \right) \quad (7)$$

For deriving the rise time of Phase B current consider the Figure. 6a

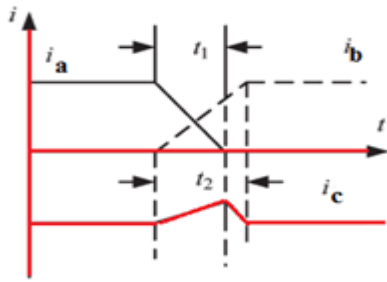


Figure 6(a).  $V_{dc} > 4E_m$

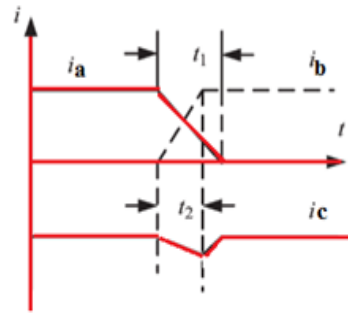


Figure 6(b).  $V_{dc} < 4E_m$

$$\begin{aligned}\frac{di_b}{dt} &= \frac{(2V_{dc} - E_m)}{3L} \\ \frac{I_m - 0}{t_1} &= \frac{(2V_{dc} - E_m)}{3L} \Rightarrow t_1 = \frac{3LI_m}{2(V_{dc} - E_m)}\end{aligned}\quad (8)$$

$$\begin{aligned}\frac{di_a}{dt} &= \frac{-(V_{dc} + 2E_m)}{3L} \\ \frac{0 - I_m}{t_2} &= \frac{-(V_{dc} + 2E_m)}{3L} \Rightarrow t_2 = \frac{3LI_m}{V_{dc} + 2E_m}\end{aligned}\quad (9)$$

Related torque ripple is given by

$$\Delta T_e = T_e - T_{e0} = \frac{V_{dc} - 4E_m}{3L} t \quad (10)$$

From (10), it is clear that in order to obtain zero torque,

$$V_{dc} - 4E_m = 0 \Rightarrow \boxed{V_{dc} = 4E_m}$$

It is known from the aforementioned analysis that by injecting a dc voltage of  $4E_m$  during commutation, it is possible to reduce commutation torque ripple to a larger extent. Hence in the present paper, by adopting proper control strategy, the duty ratio of the HBDC converter is adjusted such that the converter provides a dc voltage of  $4E_m$  during the period of commutation.

#### 4. DESIGN OF HIGH BOOST RATIO DC-DC CONVERTER FOR BLDC MOTOR DRIVE

The HBDC is a combination of flyback converter and boost converter as highlighted in Figure 7(a) and 7(b) respectively.

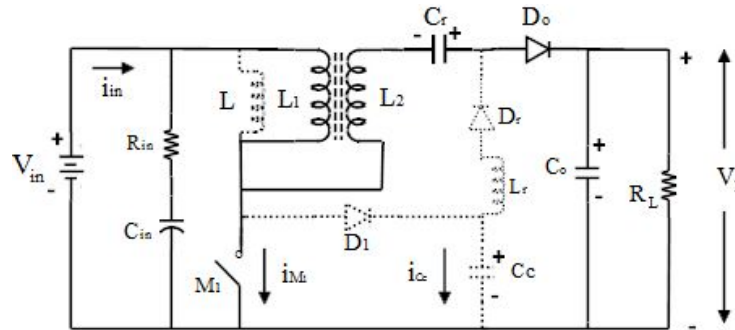


Figure 7(a). Highlighting the Flyback converter

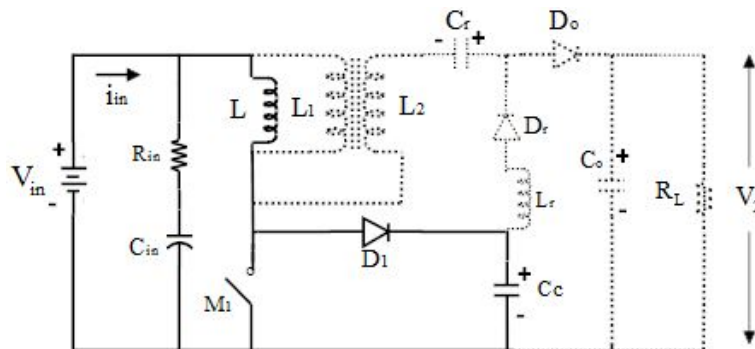


Figure 7(b). Highlighting the Boost converter

The boost converter output is stored in the clamping capacitor  $C_c$  and is expressed as in (11)

$$V_{C_c} = \frac{V_{in}}{1-D} \quad (11)$$

When the switch is ON, both  $V_{C_c}$  and the transformer output (leakage inductance) are responsible for charging of the resonant capacitor  $C_r$ . The voltage across the resonant capacitor is given by (12)

$$V_{cr} = nV_{in} + V_{C_c} \quad (12)$$

Substituting (11) in (12) gives

$$V_{cr} = \left( n + \frac{1}{1-D} \right) V_{in} \quad (13)$$

The remaining setup is that of a flyback converter and its output is given by [20]

$$V_{fo} = \left( \frac{1+nD}{1-D} \right) V_{in} \quad (14)$$

The overall output is the sum of the output of the flyback converter and the voltage across the resonant capacitor which is in series with it. The effective DC output is

$$V_{dc} = \left( \frac{1+nD}{1-D} \right) V_{in} + V_{Cr} \quad (15)$$

Substituting (13) in (15)

$$V_{dc} = \left( \frac{n+2}{1-D} \right) V_{in}$$

Hence the duty ratio is

$$D = 1 - (n+2) \frac{V_{in}}{V_{dc}} \quad (16)$$

As per (10), during commutation it is desired to have  $V_{dc} = 4E_m$ . Hence during commutation the duty ratio of HBDC should be adjusted as

$$D = 1 - (n+2) \frac{V_{in}}{4E_m} \quad (17)$$

## 5. CONTROL OF HIGH BOOST RATIO DC-DC CONVERTER FED BLDC MOTOR DRIVE

Figure 8 shows the block diagram of the closed loop control system of the BLDC motor.

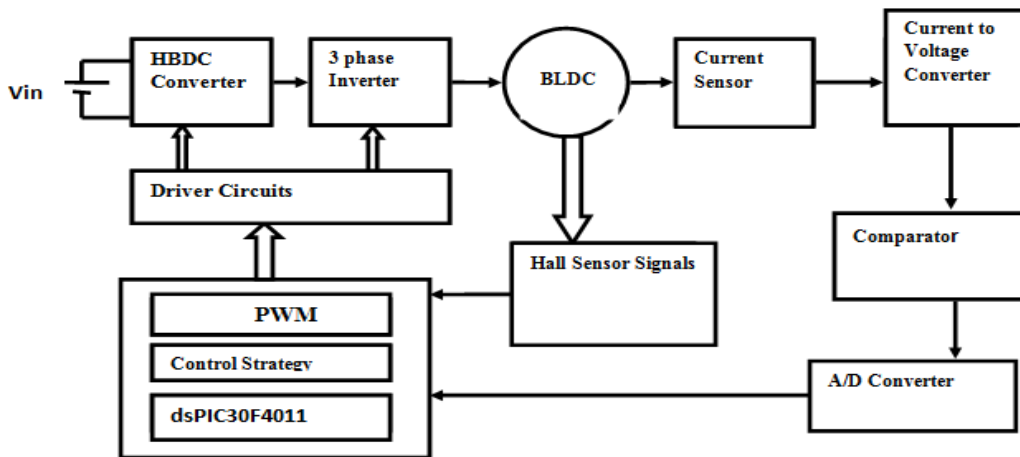


Figure 8. Control system of the BLDC motor

A three-phase motor rated 160W, 48 Vdc, 3000 rpm is fed by a HBDC and six step voltage source inverter. The inverter gates signals are produced by decoding the Hall Effect signals of the motor. The three-phase output of the inverter is applied to the BLDC motor stator windings. Two control loops is used. The inner loop synchronizes the inverter gates signals with the help of Hall sensors. The outer loop compares the stator current of the motor and regulates to vary the output of the high boost ratio DC-DC Converter by suitably adjusting the duty ratio of the Converter.



As mentioned earlier, the torque ripples are prominent during the commutation period. A high voltage input ( $4E_m$ ) is to be injected to the inverter during that period [16]. Instead of using two different converters or an additional voltage source as given in [17], it is advantageous to vary the output of the DC-DC converter by suitably adjusting the duty ratio of the converter. Hence an arrangement is required to detect the commutation period of the BLDC motor. Figure 9 shows the control arrangement for detecting the commutation period.

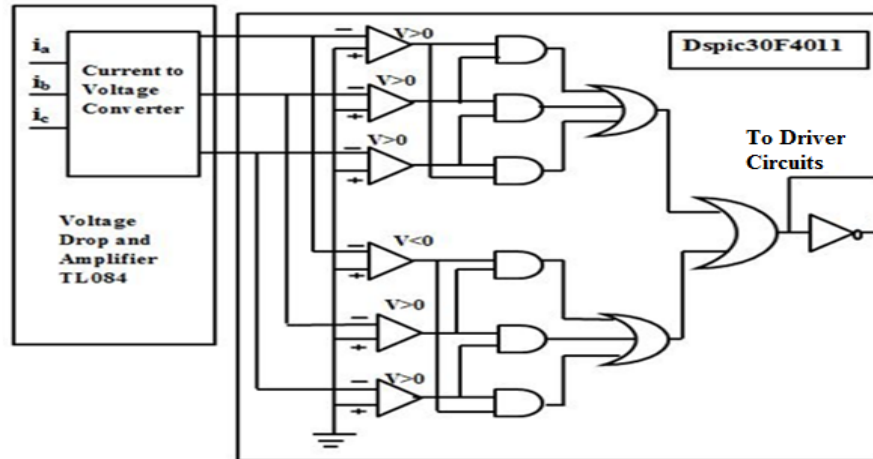


Figure 9. Schematic representing Digital signal controller functionalities

Signals from the Hall sensors and the stator phase currents are given as input to the control scheme wherein the first stage a current to voltage converter is used. An operational amplifier in comparator mode is used with one of the inputs grounded. Only during commutation period two of the phases have the same polarity (owing to the presence of a cross-over between two phases in either polarity), which can be detected using AND gates. This signal is used to adjust the duty ratio of the converter. The digital logic circuit used in the control scheme generates HIGH output when commutation occurs and LOW when non-commutation period.

## 6. SIMULATION AND EXPERIMENTAL RESULTS

In order to assess the performance of the system with a particular focus on commutation torque ripple, a Matlab-Simulink based model in time domain has been developed. The output performances are current, voltage, back-EMF, and the torque variation under steady-state operating conditions.

The simulated and experimental waveform of the BLDCM drive system with the proposed HBDC converter at 1500 rpm is shown in Figure 10 to Figure 13. The simulated output voltage of the high boost ratio DC-DC converter is shown in Figure 10(a) and the corresponding experimental waveform is shown in Figure 10(c). It can be seen that  $V_{dc} = 4E_m$  under the appropriate input voltage of the inverter during commutation period, the torque ripple during commutation is proportional to  $|V_{dc} - 4E_m|$ ,  $V_{dc}$  is closer to  $4E_m$  torque pulsation is significantly reduced. The simulated Inverter line to line voltage is shown in Figure 10(b) and the corresponding experimental waveform is shown in Figure 10(d). It can be seen that the input of the inverter dc link voltage during commutation period the rising and falling portion of corresponding line voltage is affected by spikes.

The duty ratio of HBDC is appropriately controlled in order to inject a  $V_{dc}$  of  $4E_m$  during commutation an additional voltage of 160 volts is injected. In dc link during chopping period the rising and falling period of corresponding line voltage is affected by spikes. The simulated and experimental results for stator current of BLDC motor are shown in Figure 11 and Figure 12 respectively. In these, the places marked with circle shows that the current slopes of incoming and outgoing phases during commutation through the recommended method are far closer than those without commutation [17]. The spikes of which currents occurring at the end of commutation get smooth, and the current is much closer to a rectangle.

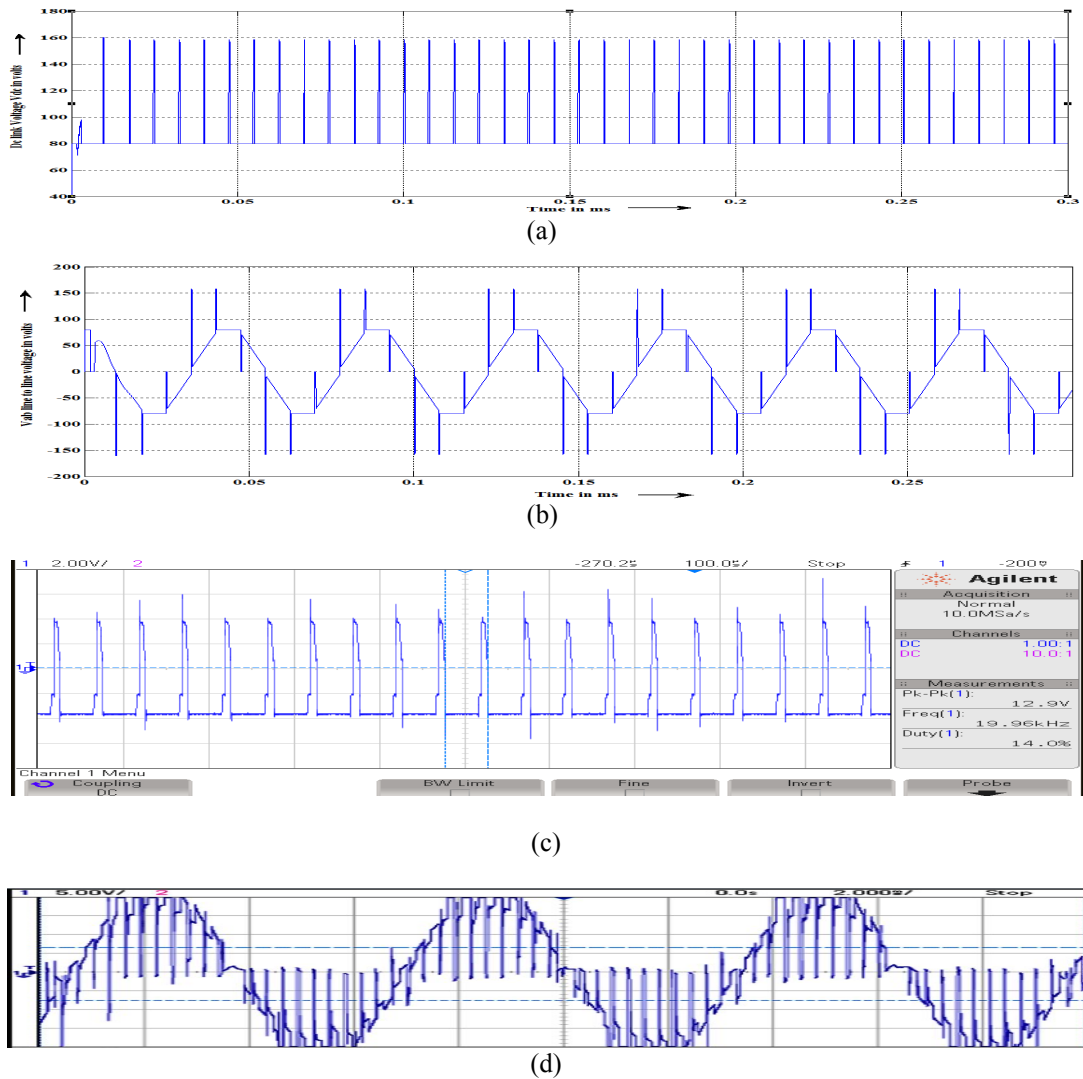


Figure 10. The simulated and experimental waveform of the BLDCM drive system; (a). Simulated result for output voltage of the high boost ratio DC-DC converter. (b) Simulated result for Inverter line to line voltage. (c) Experimental result for output voltage of the high boost ratio DC-DC converter. (d) Experimental result for Inverter line to line voltage.

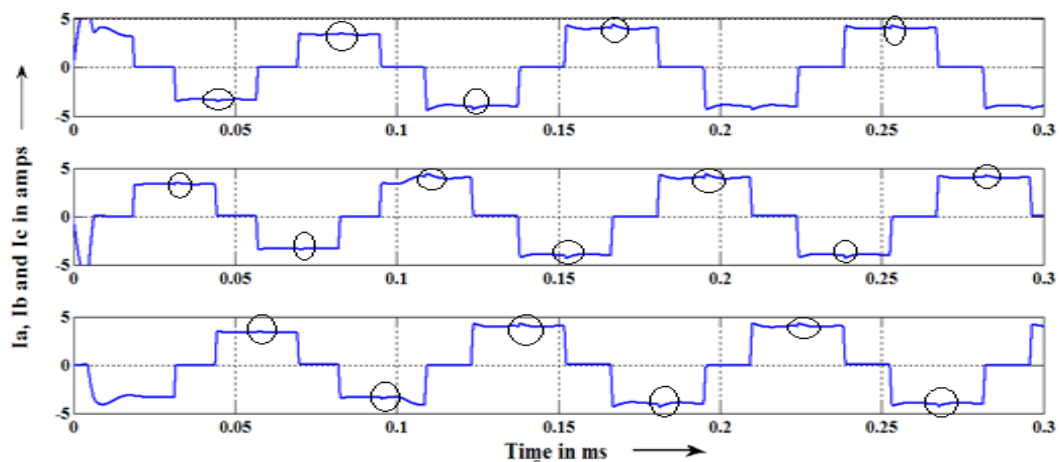
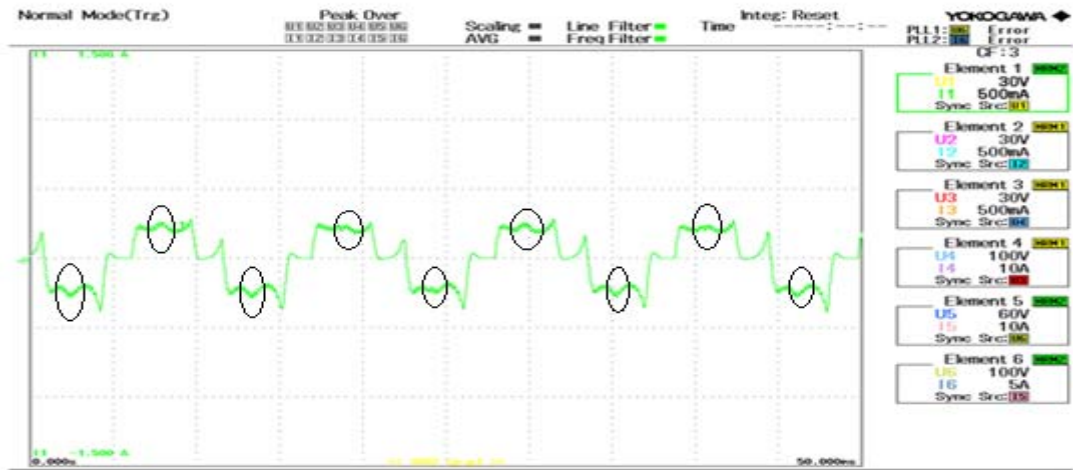
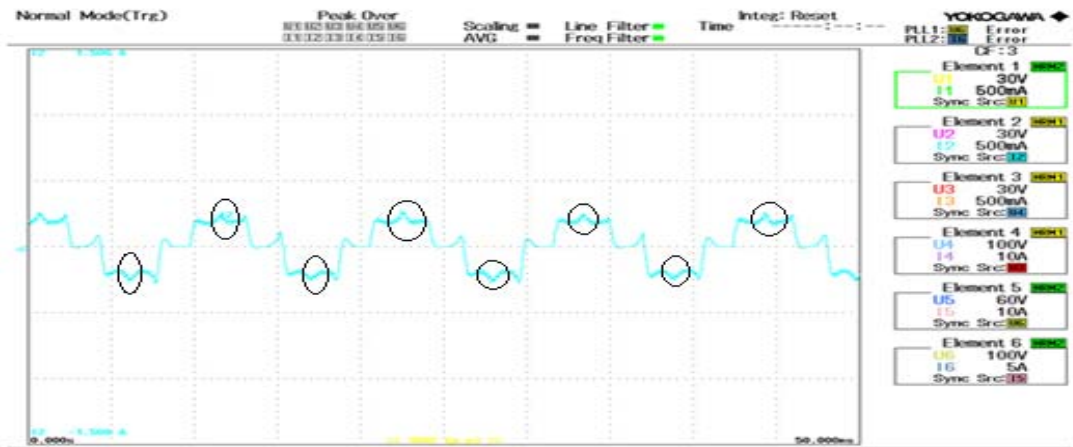


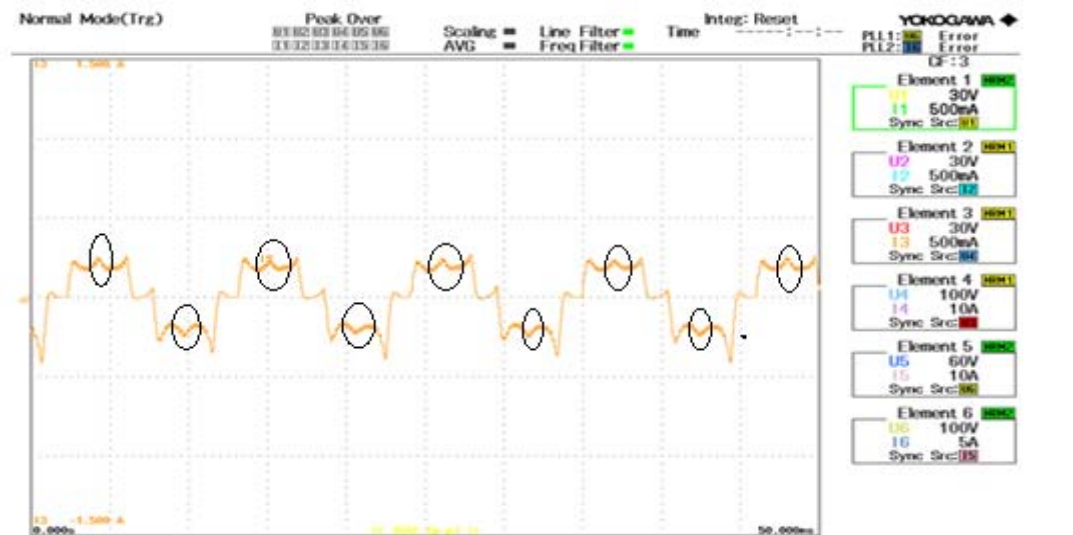
Figure 11 Stator current of all the three phases of BLDC motor



(a)



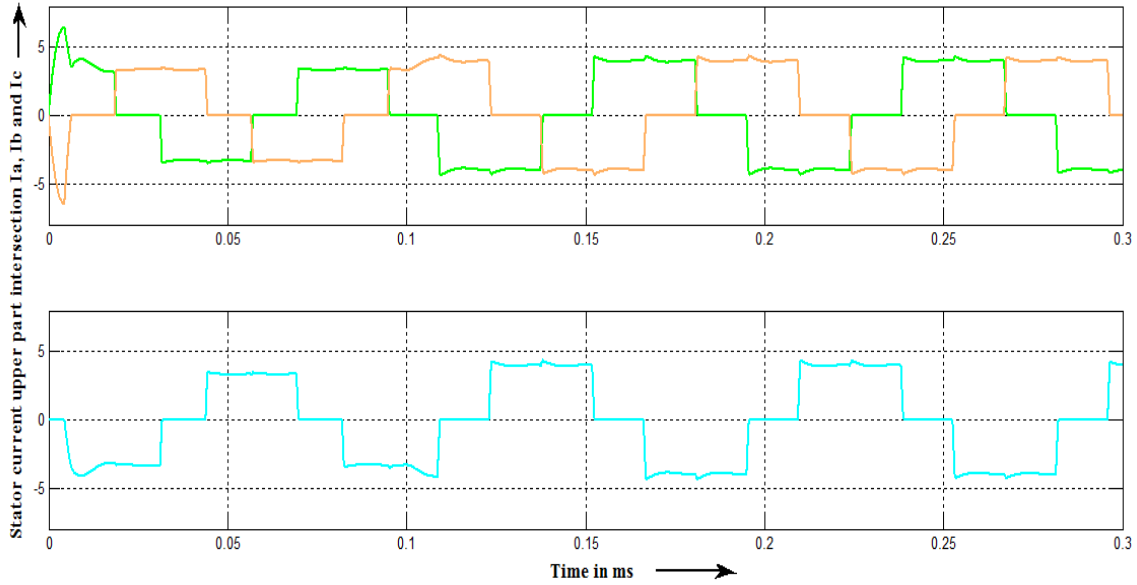
(b)



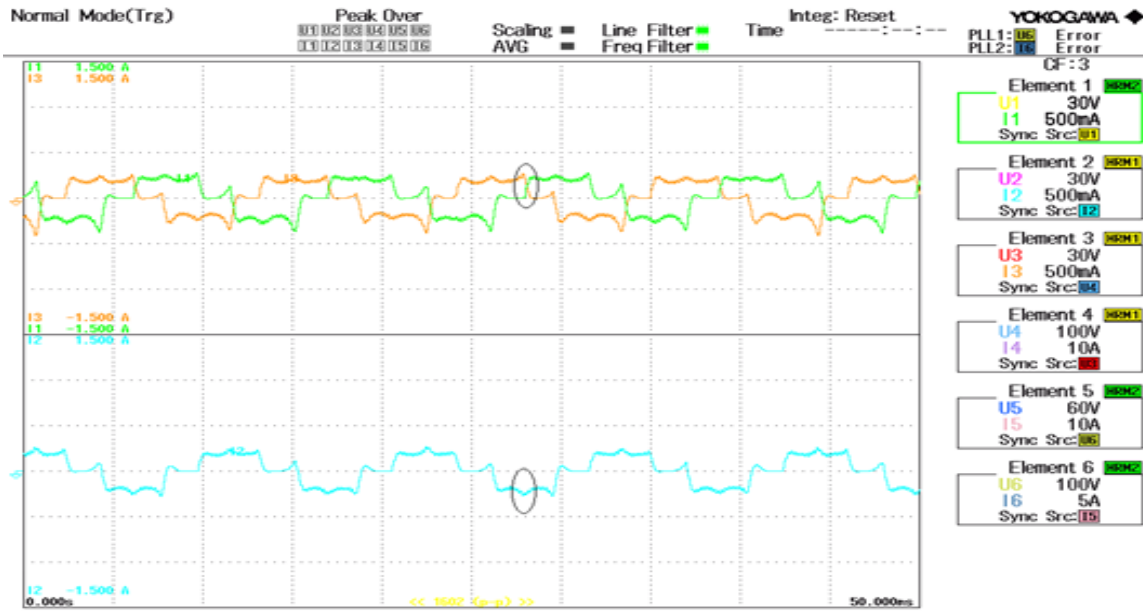
(c)

Figure 12 . The simulated and experimental of the BLDCM drive system; (a) Experimental result for Stator phase A current. (b) Experimental result for Stator phase B current. (c) Experimental result for Stator phase C current.

Though phase current and electromagnetic torque is different, the electromagnetic torque of BLDC motor is proportional to the phase current, the waveforms of phase current can be treated as the estimated waveform of the output torque of the motor. Thus from the phase current shape, we can approximate the output torque shape. The rising current and falling current are matched, and the corresponding duration is significantly reduced as shown in Figure.11. and Figure.12. Also the non commutated phase current is almost constant during this period and hence commutation torque ripple is significantly reduced.



(a)



(b)

Figure 13 . The simulated and experimental of the BLDCM drive system; (a) Simulated result for upper part intersection of Stator Current. (b) Experimental result for upper part intersection of Stator current

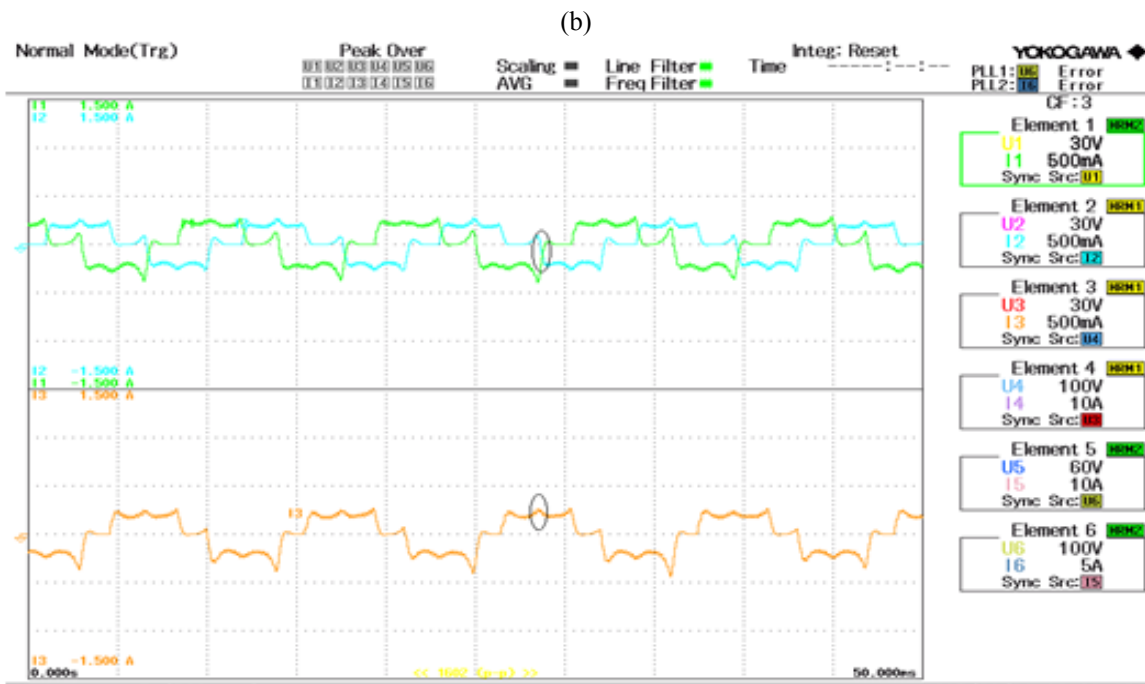
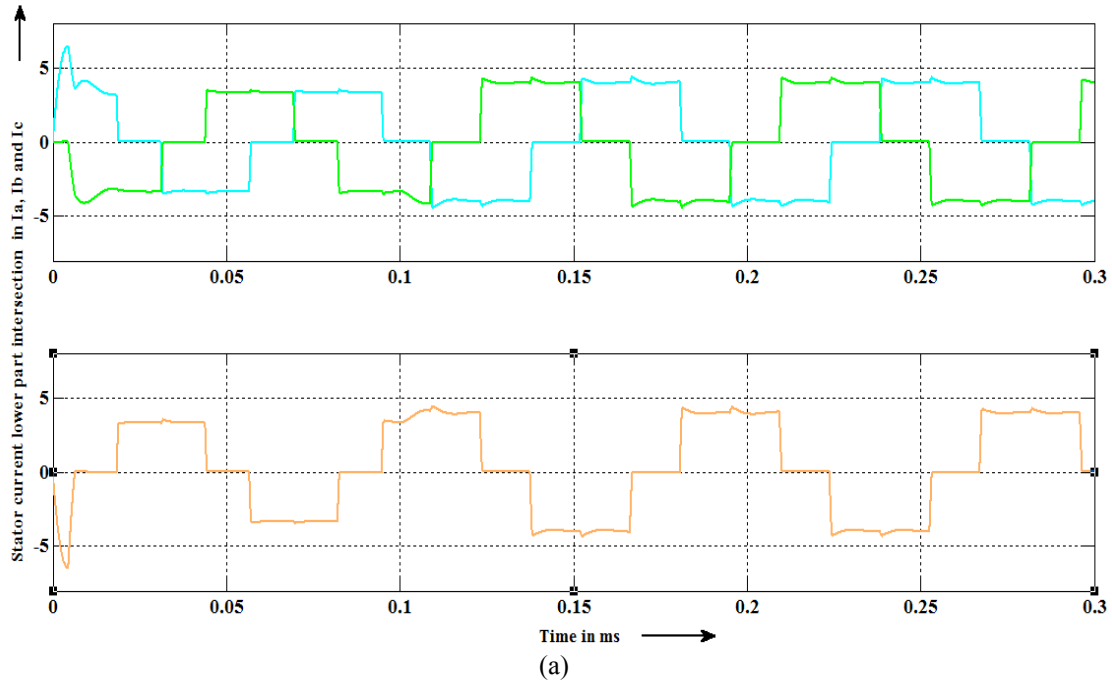


Figure 14. The simulated and experimental of the BLDCM drive system; (a). Simulated result for upper part intersection of Stator Current. (b) Experimental result for upper part intersection of Stator current.

The current behaviours with lower part and upper part intersection for simulated and experimental results are shown in Figure.13 and Figure.14. The slopes of the currents during commutation depend on the dc link voltage  $V_{dc}$  and the maximum value of back EMF  $E_m$ .  $E_m$  is proportional to speed and considered constant during commutation.  $V_{dc}$  is generally variable due to controllable HBDC converter.  $V_{dc} = 4E_m$  cannot always be satisfied, which leads to significant torque ripples. In the torque ripple analyses during commutation is proportional to  $V_{dc} = 4E_m$ , at the commutation to non-commutation interval, the little torque ripple becomes. In this paper, a new HBDC converter is proposed, which can reduce commutation torque ripples by keeping  $V_{dc}$  close to  $4E_m$  during commutation.

Two back-EMF sensing methods for the PM BLDC motors available in literature, which are direct and indirect back-EMF detection methods [19]. In direct back-EMF detection methods, its zero crossing is detected by comparing it with neutral point voltage. It suffers from high common mode voltage and high frequency noise due to the PWM drive, so it needs low pass filters, and voltage dividers. Indirect back-EMF detection methods are because filtering introduces commutation delay at high speeds and attenuation causes reduction in signal sensitivity at low speeds, the speed range is narrowed in direct back-EMF detection methods. In order to reduce switching noise, the indirect back-EMF detection methods are used [19]. The indirect back-EMF detection methods namely Back-EMF Integration and Third Harmonic Voltage Integration. These are found to be complex; hence in this paper a new method called terminal current sensing (phase current commutation) method has been adopted.

In order to validate the simulation results, and hence to show the effectiveness of the proposed modelling, an experimental system has been built. This system is composed of a BLDC motor fed through a three-phase voltage inverter whose inputs are controlled by the proposed HBDC. The details of the motor are given in the Appendix.

The control and the digital signal functions are as shown in Fig.8 and Fig.9. Output pulses from the high performance 16-bit digital signal controller dsPIC30F4011 are fed into pulse driver IR2110. The MOSFETs used in the power circuit are IRF840 with 500V, 8A rating. Figure.15. highlights the components used in the testing bed. Also, a digital storage oscilloscope has been used for storing the waveforms of the back emf and phase currents.

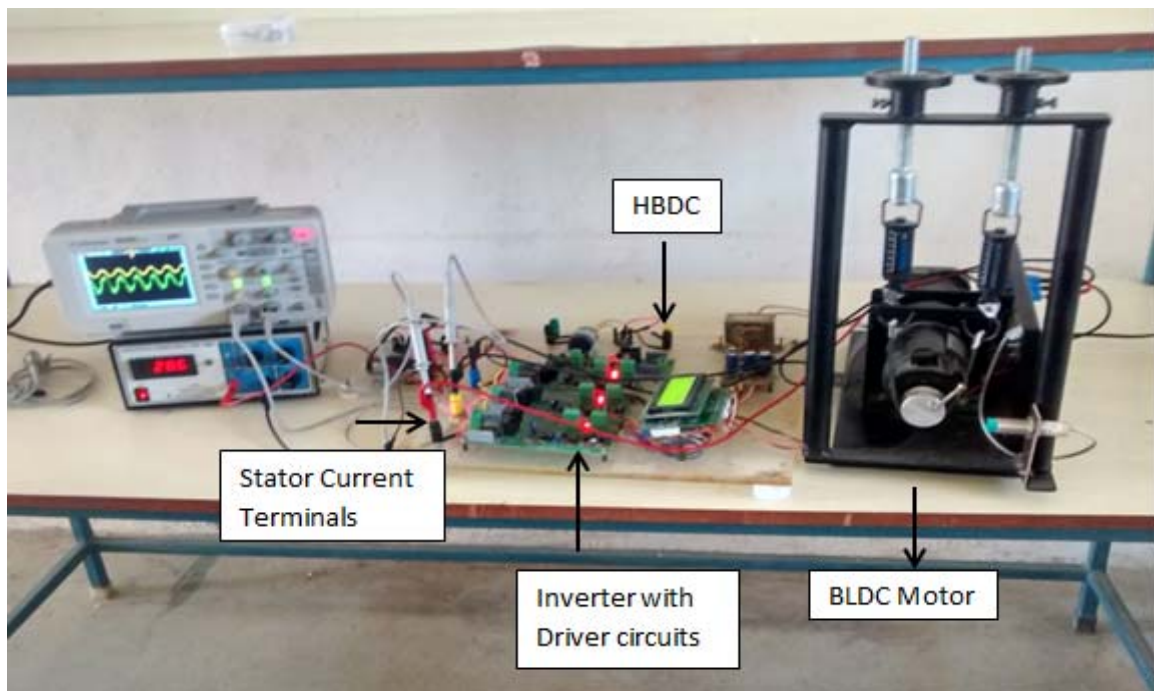


Figure 15. Experimental Setup

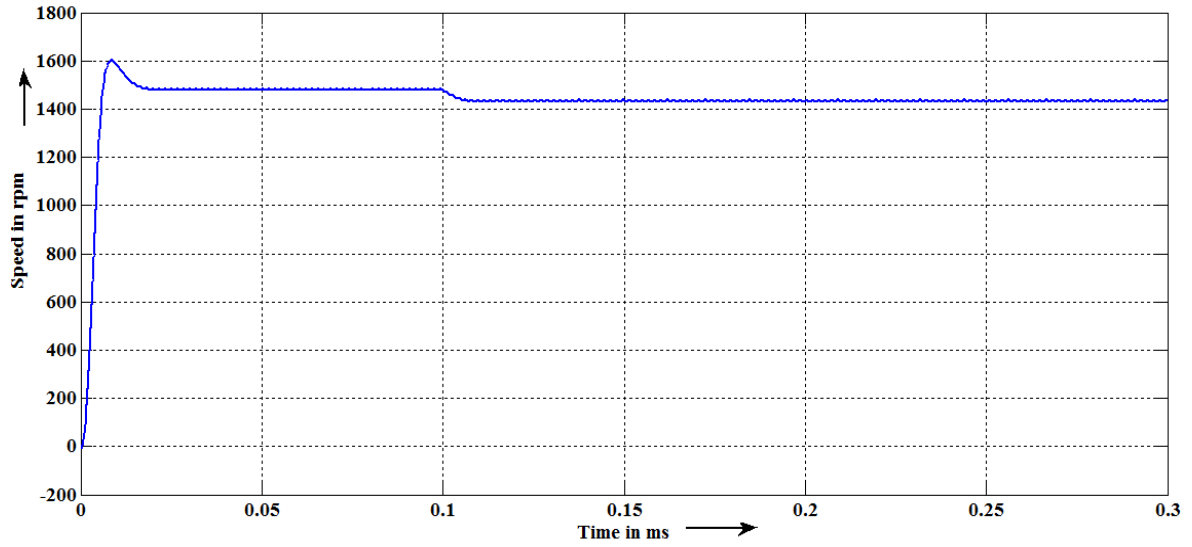


Figure 16(a). Measured Speed with traditional six-step control method

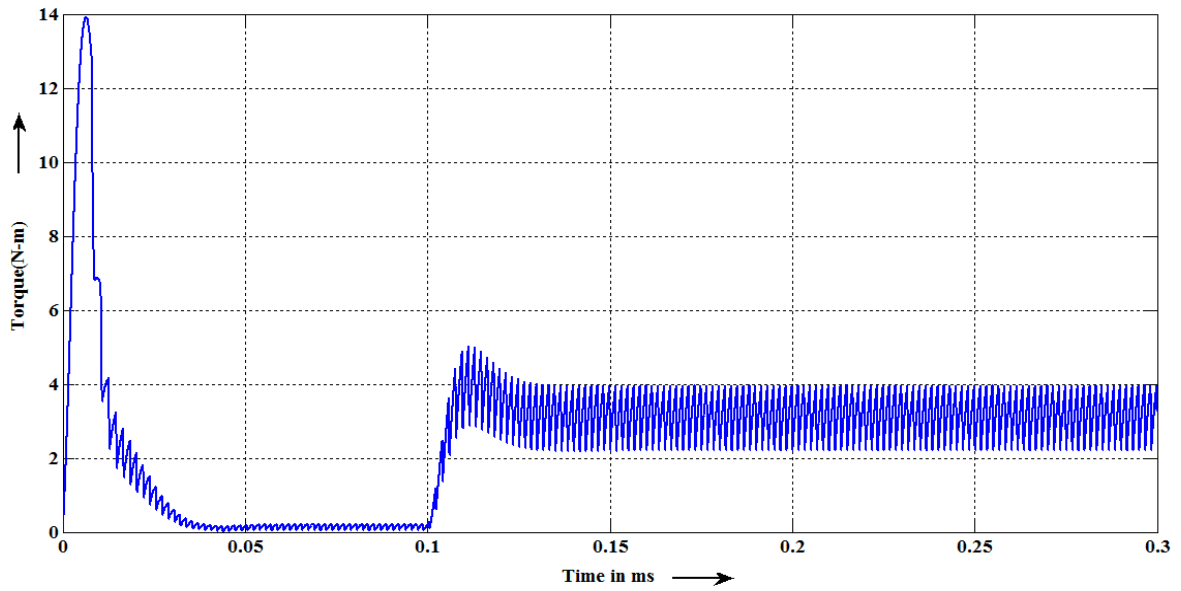


Figure 16 (b). Measured Torque with traditional six-step control method

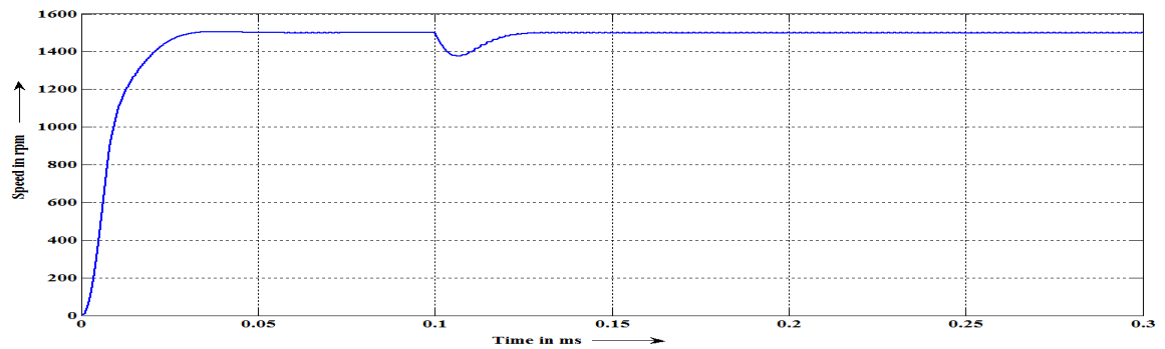


Figure 17(a). Measured Speed with High Boost Ratio DC-DC Converter

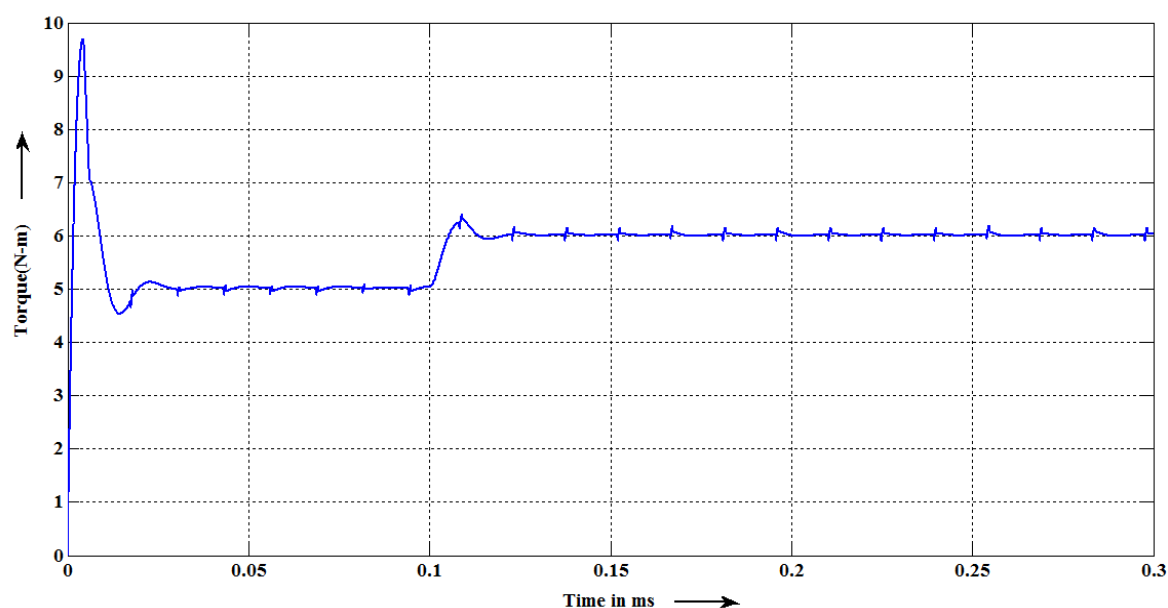


Figure 17(b). Measured Torque with High Boost Ratio DC-DC Converter

Figure 10 to Figure 17 present respectively the simulation and the experimental results of the motor phase current for a speed of 1500 rpm and it is revealed from these plots the simulated and the experimental results are very close.

As shown by some researcher presented in [15] - [17], speed response, phase current and torque are compared between the conventional six-step method and the dc link voltage strategy. In [17] SEPIC converter is used, and commutational torque ripple is reduced. It can be calculated that the torque ripples decreases from 48.1% to 19.5%.

In this paper, a novel topology of a High Boost Ratio DC-DC Converter is proposed, figure.17 shows the simulated torque and it can be seen that under the appropriate input voltage fed by the HBDC to the inverter during commutation, torque pulsation is significantly reduced and the resultant electromagnetic torque waveform is more uniform compared with electromagnetic obtained in the traditional six-step control method. It can be calculated that torque ripple decreases from about 48.1% to 10.2% at the rated speed.

## 7. CONCLUSION

Torque ripple reduction is a necessary requirement for high performance BLDC motor drives. The phase commutation is one of the major causes of torque ripple generation in a BLDC machine. In this paper, a high boost ratio DC-DC converter with a very low dc input voltage is proposed in the front end of the inverter. The DC-DC converter is operated with a suitable control strategy for providing excess voltage from the same converter during commutation, which enables to drive phase currents to increase and decrease in the identical slope, resulting in the great reduction of pulsated commutation torque. Experimental results were presented to validate the simulated results. The results indicate that the proposed approach exhibits improved performance for reducing the commutation torque ripple.

### Appendix

BLDC Motor Rating	
DC Voltage	= 50 V
Rated power	= 120W
Phase resistance	= 1 $\Omega$
Phase inductance	= 1.8mH
Rated speed	= 1500 rpm
No of poles	= 4
Rated Torque	= 1.2 Nm
PWM Switching frequency	= 20KHz



## REFERENCES

- [1] A. Sathyan, N. Milivojevic, Y.-J. Lee, M. Krishnamurthy, and A. Emadi, "An FPGA-based novel digital PWM control scheme for BLDC motor drives," *IEEE Trans. Ind. Electron.*, vol. 56, no. 8, pp. 3040–3049, Aug. 2009.
- [2] G. J. Su and J. W. Mckeever, "Low-cost sensorless control of brushless DC motors with improved speed range," *IEEE Trans. Power Electron.*, vol. 19, no. 2, pp. 296–302, Mar. 2004.
- [3] S.S. Bharatkar, R. Yanamshetti, D. Chatterjee, and A.K. Ganguli, "Dual-mode switching technique for reduction of commutation torque ripple of brushless dc motor", *IET Electr. Power Appl.*, 2011, Vol. 5, Iss.no 1, pp. 193–202.
- [4] F. Rodriguez and A. Emadi, "A novel digital control technique for brushless dc motor drives," *IEEE Trans. Ind. Electron.*, vol. 54, no. 5, pp. 2365–2373, Oct. 2007.
- [5] C.-T. Pan and E. Fang, "A phase-locked-loop-assisted internal model adjustable-speed controller for BLDC motors," *IEEE Trans. Ind. Electron.*, vol. 55, no. 9, pp. 3415–3425, Sep. 2008.
- [6] C. Xia, Z. Li, and T. Shi, "A control strategy for four-switch three-phase brushless dc motor using single current sensor," *IEEE Trans. Ind. Electron.*, vol. 56, no. 6, pp. 2058–2066, Jun. 2009.
- [7] Jian Shi and Tie-Cai Li, "New Method to Eliminate Commutation TorqueRipple of Brushless DC Motor with Minimum Commutation Time", *IEEE Trans. Ind. Electron.*, vol. 60, no. 6, pp. 6, Jun. 2013
- [8] R. Krishnan, *Electric Motor Drives: Modeling, Analysis and Control*, Pearson Education, India, 2001.
- [9] T. M. Jahns and W. L. Soong, "Pulsating torque minimization techniques for permanent magnet ac motor drives—A review," *IEEE Trans. Ind. Electron.*, vol. 43, no. 2, pp. 321–330, Apr. 1996.
- [10] S. J. Park, H.W. Park, M. H. Lee, and F. Harashima, "A new approach for minimum-torque-ripple maximum-efficiency control of BLDC motor," *IEEE Trans. Ind. Electron.*, vol. 47, no. 1, pp. 109–114, Feb. 2000.
- [11] L. Parsa and L. Hao, "Interior permanent magnet motors with reduced torque pulsation," *IEEE Trans. Ind. Electron.*, vol. 55, no. 2, pp. 602–609, Feb. 2008.
- [12] R. Carlson, L.-M. Milchel, and J. C. Fagundes, "Analysis of torque ripple due to phase commutation in brushless dc machines," *IEEE Trans. Ind. Appl.*, vol. 28, no. 3, pp. 632–638, May/June 1992.
- [13] S.I. Kim, J.Y. Lee, Y.K. Kim, J.P. Hong, Y. Hur and Y.H. Jung, "Optimization for reduction of torque ripple in interior permanent magnet motor by using Taguchi method", *IEEE Trans. Magn.*, vol. 41, no. 5, pp. 1796–1799.
- [14] B. Boukais and H. Zeroug, "Magnet segmentation for commutation torque ripple reduction in a brushless dc motor drive," *IEEE Trans. Magn.*, vol. 46, no. 11, pp. 3909–3919, Nov. 2010.
- [15] X. F. Zhang and Z. Y. Lu, "A new BLDC motor drives method based on BUCK converter for torque ripple reduction," in *Proc. IEEE Power Electron. Motion Control, Conf.*, 2006, pp. 1–4.
- [16] W. Chen, C. L. Xia, and M. Xue, "A torque ripple suppression circuit for brushless DC motors based on power dc/dc converters," in *Proc. IEEE Ind. Electron. Appl., Conf.*, 2008, pp. 1453–1457.
- [17] Tingna Shi, Yuntao Guo, Peng Song, and Changliang Xia, "A New Approach of Minimizing Commutation Torque Ripple for Brushless DC Motor Based on DC–DC Converter", *IEEE Transactions on Industrial Electronics*, VOL. 57, NO. 10, OCTOBER 2010
- [18] W. H. Li and X. N. He, "Review of non-isolated high step-up DC/DC converters in photovoltaic grid-connected applications," *IEEE Trans. Ind. Electron.*, vol. 58, no. 4, pp. 1239–1250, Apr. 2011
- [19] Sanjeev Singh. "PFC buck-boost converter based voltage controlled adjustable speed PMBLDCM drive for air-conditioning", *European Transactions on Electrical Power*, 2010 Volume 21, Issue 1, pages 424–438, January 2011
- [20] T. Raghu, S. Chandra Sekhar, J. Srinivas Rao " SEPIC Converter based-Drive for Unipolar BLDC Motor ", *International Journal of Electrical and Computer Engineering (IJECE)*, Vol.2, No.2, pp. 159~165, ISSN: 2088-8708, April 2012
- [21] Pritha Agrawal, Satya Prakash Dubey, Satyadhama Bharti. " Comparative Study of Fuzzy Logic Based Speed Control of Multilevel Inverter fed Brushless DC Motor Drive ", *International Journal of Power Electronics and Drive System (IJPEDS)*, Vol. 4, No. 1, pp. 70~80, ISSN: 2088-8694, March 2014

## BIOGRAPHIES OF AUTHORS



M. Senthil Raja was born in Tamilnadu, India in 1981. He received the B.E degree in Electronics & Communication Engineering from Anna University in 2005, the M.E degree in Power Electronics & Drives from Anna University in 2011. He is currently research scholar in Pondicherry University. His research interests include power converter and electrical drives.



Dr. B. Geethalakshmi. She received the B.E degree in Electronics & Communication Engineering from Bharathidasan University in 1996 , the M.E. degree in Power Electronics & Drives from Bharathidasan University in 1999, and the Ph.D.degree in FACTS controllers from Pondicherry University in 2009. She is currently an Associate Professor under the department of Electrical & Electronics Engineering in Pondicherry Engineering College. Her current research interests include FACTS controller, power electronics, and motor drives.